Chen, A. S., Herrmann, G., Na, J., Turner, M., Vorraro, G., & Brace, C. (2018). Nonlinear Observer-Based Air-Fuel Ratio Control for Port Fuel Injected Wankel Engines. In *2018 UKACC 12th International Conference on Control (CONTROL 2018): Proceedings of a meeting held 5-7 September 2018, Sheffield, United Kingdom* (pp. 224-229). Institute of Electrical and Electronics Engineers (IEEE). https://doi.org/10.1109/CONTROL.2018.8516842

Nonlinear Observer-Based Air-Fuel Ratio Control for Port Fuel Injected Wankel Engines

Anthony Siming Chen, Guido Herrmann, Jing Na, Matthew Turner, Giovanni Vorraro, and Chris Brace

***Abstract*—The use of Wankel engines has been severely limited as the emission regulations get stringent around the world since the 1970s. The fuel puddles due to port fuel injection (PFI) and the leakage between combustion chambers are significant sources of efficiency loss and emissions. For most spark ignition engines in production, the emission strongly depends on the air-fuel ratio (AFR) controller in cooperation with a three-way catalytic (TWC) converter. This paper presents a generic observer-based AFR control framework to deal with the high nonlinearities of Wankel engines so as to improve the fuel economy and emissions. By taking the unknown parameters as augmented engine states, an extended Kalman filter is designed to estimate the fuel puddle dynamics using only mass air flow (MAF) and lambda sensors. The complex nonlinear air-filling dynamics are lumped together and estimated using novel observer techniques. A newly proposed unknown input observer is compared with a dirty differentiation observer and then employed in the feedback AFR control design. Comparative simulations based on a calibrated benchmark engine model show that the proposed control can speed up the transient response and regulate the AFR around the stoichiometric value.**

***Index Terms*—engine control, nonlinear observer, air-fuel ratio, port fuel injection, wankel engine, Kalman filter, engine modelling**

I. Introduction

Recently, the idea of incorporating a Wankel engine as range extenders for electric vehicles has been proposed due to its compact design and high power-weight ratio, which directly stimulates the renewed investigations on Wankel engine control [1]. Unlike one power pulse per two revolutions in four-stroke reciprocating engines, Wankel rotary engines generate three power pulses per revolution, which delivers advantages of high revolutions per minutes and smoothness [2]. However, the shortcoming of high emissions has severely limited the application of Wankel engines in the automotive industry. The major Wankel engine producer Mazda ceased the last production of the RX-8 in 2012. Nowadays, its application prevails only in bespoke areas such as unmanned aerial vehicles (UAVs) and auxiliary power units [3]. The main cause of the high emissions of Wankel engines is given by its design. On the one hand, the significantly different temperatures in each combustion chamber often lead to imperfect sealing, which accounts for leakage and unburned fuel mixture [4]. On the other hand, it is inevitable for port fuel injection (PFI) that a considerable portion of fuel will be trapped at the intake manifold wall as fuel puddles, which is also known as the "wall-wetting" phenomenon. One way to overcome this is implementing direct fuel injection (DFI) into the combustion chambers, which has proved successful for reciprocating compression ignition engines and then in reciprocating spark ignition engines [1]. However, the implementation of DFI is likely to increase the cost and the complexity of engine configurations. Alternatively, one can design an air-fuel ratio (AFR) controller using observers to compensate for the effect of fuel puddle dynamics and for the rapid change of air-filling dynamics.

The common treatment for engine emissions is to convert pollutant exhaust gases (CO, NO_x) into innocuous ones (N_2, H_2O and CO_2) using three-way catalytic (TWC) converters. However, the conversion efficiency of TWC is fairly sensitive to AFR, which is required to be regulated around the stoichiometric value (e.g. 14.67 for petrol) [5]. Moreover, combustion with a stoichiometric AFR is essential to achieving the optimal thermal efficiency and dynamic performance. Therefore, it is of great importance to design a well-performing AFR controller for Wankel engines so as to improve emissions, thermal efficiency and fuel economy. For most spark ignition engines in production, the widely-used control strategy is still PID control based on lookup tables, which could be difficult to meet the emission requirement in the presence of complex dynamics and rapid-change operation scenarios of Wankel engines. Practically, the compilation of the lookup tables also requires significant effort in engine calibration tests and is usually time-consuming [6].

This motivates the research on advanced AFR control design such as optimal control [7], robust control [8][9], adaptive control [5][10], and more recently, observer-based control [6][11]. An optimal AFR controller was designed in [7] considering the cyclic variations of residual gas. However, it requires the knowledge of in-cylinder pressure, for which the sensor could often be expensive and not applicable for commercial engines. Then, robust techniques such as H_∞ control [8] and sliding mode control [9] were proposed to regulate the AFR in the presense of external disturbance. In order to deal with parameter uncertainties, adaptive approaches were presented to address air-filling dynamics in [5] and time delay dynamics in [10]. However, the complexity of the adaptive controller limits their practical implementation. This prompts further work on the AFR control using simple, easily implemented observers. In [11], a sliding mode AFR controller was proposed using

A.S. Chen is with the Department of Mechanical Engineering, University of Bristol, BS8 ITR, UK. (E-mail: Anthony.Chen@bristol.ac.uk)

G. Herrmann is with the Department of Mechanical Engineering, University of Bristol, BS8 ITR, UK. (E-mail: G.Herrmann@bristol.ac.uk)

J. Na is with the Faculty of Mechanical and Electrical Engineering, Kunming University of Science and Technology, Kunming, China

M. Turner, G. Vorraro and C. Brace are with the Powertrain and Vehicle Research Centre, University of Bath, BA2 7AY, UK.

observers to reduce chattering. Later on, various popular observer techniques were investigated in [6], which show great potential in application with design simplicity. However, the effect of fuel puddle dynamics was not specifically studied in [6]. There the two parameters: fuel puddle fraction and the time constant for the puddle evaporation, are assumed to be known for AFR control, which are, however, not measurable in practice.

In this paper, in order to design a simple yet robust AFR controller for Wankel engines, a mean-value engine model is developed. Moreover, this paper incorporates the idea of an extended Kalman filter [12] to account for the effect of fuel puddle dynamics. By reformulating the AFR regulation into a fuel flow tracking problem, various popular observer techniques [6] are investigated and employed in the AFR control design, which leads to a new observer-based AFR control framework. Comparative simulations present the improved transient and steady-state responses.

II. Wankel Engine Dynamics

This section describes a zero-dimension model of the port fuel injected Wankel engine dynamics. There has been a large number of studies (e.g. the mean-value engine model (MVEM) developed by Hendricks [13][14]) on the dynamics of reciprocating engines whereas few on the modelling of Wankel engines (e.g. [4][2][15] around the early 1980s). However, it is feasible to model the Wankel engine using an equivalent reciprocating MVEM since it operates with the same Otto cycle, i.e. a single rotor Wankel engine is equivalent to a two-cylinder four-stroke reciprocating engine [4].

A. Intake Air flow model

The air mass flow rate $\dot{m}_{at}$ passing the throttle can be described [13] as

$$\dot{m}_{at}(\alpha, p_m) = m_{at1}\frac{p_a}{\sqrt{T_a}}TC(\alpha)PRI(p_m) + m_{at0} \tag{1}$$

where $m_{at1} = c_t\frac{\pi}{4}D^2\sqrt{2\kappa/R(\kappa-1)}$ is a physical constant related to the ratio of the specific heats κ, the gas constant R, the flow coefficient c_t and the diameter D of throttle body throat; m_{at0} is a fitting constant; p_a and T_a are the ambient pressure and temperature, respectively; $TC(\alpha) = 1 - cos(\alpha - \alpha_0)$ denotes the throttle characteristics function of the throttle plate angle α and the leakage constant α_0, which approximates the effective throttle area; $PRI(p_m)$ refers to the pressure ratio influence from the choke/sonic compressible flow, which can be expressed as

$$PRI(p_m) = \begin{cases} \sqrt{1 - (\frac{p_r - p_c}{1 - p_c})^2} & \text{if } p_r \geq p_c \text{ (choked)} \\ 1 & \text{if } p_r < p_c \text{ (sonic)} \end{cases} \tag{2}$$

where p_c is the threshold point and $p_r = p_m/p_a$ is the ratio of the intake manifold pressure p_m to the ambient pressure p_a. Neglecting the heat transfer [14], an adiabatic model of the air-filling dynamics in the intake manifold can be given as

$$\dot{p}_m = \frac{\kappa R}{V_m}(\dot{m}_{at}T_a - \dot{m}_a T_m) \tag{3}$$

$$\dot{T}_m = \frac{RT_m}{p_m V_m}[\dot{m}_{at}(T_a\kappa - T_m) - \dot{m}_a(T_m\kappa - T_m)] \tag{4}$$

where T_m is the manifold temperature and V_m is the manifold volume. Then the port air mass rate $\dot{m}_a$ can be given as a nonlinear function of the manifold pressure p_m and engine speed n such that

$$\dot{m}_a(p_m, n) = \frac{V_d}{120RT_m}\eta_{vol}(p_m, n)p_m n \tag{5}$$

where V_d is the engine displacement and η_{vol} is the volumetric efficiency.

B. Fuel puddle model

Due to the "wall-wetting" phenomenon, the final fuel flow rate $\dot{m}_f$ is the sum of the fuel puddle flow rate $\dot{m}_{fpe}$ and the fuel vapour flow rate $\dot{m}_{fve}$ entering the combustion chamber

$$\dot{m}_f = \dot{m}_{fpe} + \dot{m}_{fve} = m_{fp}/\tau_p + m_{fv}/\tau_m \tag{6}$$

where τ_p and τ_m are the characteristic manifold time constant for the puddle m_{fp} and vapour m_{fv} fuel mass, respectively [16]. Their dynamics can be taken as a set of two first-order processes with time constant τ as

$$\begin{cases} \dot{m}_{fp} = \chi\dot{m}_{fi} - (1/\tau)m_{fp} - \dot{m}_{fpe} \\ \dot{m}_{fv} = (1-\chi)\dot{m}_{fi} + (1/\tau)m_{fp} - m_{fv}/\tau_m \end{cases} \tag{7}$$

where $\dot{m}_{fi}$ is the injected fuel flow rate (i.e. the control command for the fuel injector) and χ, $0 \leq \chi < 1$, is a fraction of injected fuel that deposited on the manifold wall as fuel puddles. It should be noted that the fuel puddle model (6)(7) is perceived to be more correct compared to our previous version in [5] since it considers the effect of the fuel puddle flow (Couette flow) entering the chamber.

C. Combustion model

A significant feature in the combustion dynamics of Wankel engines is the leakage and the crevice volume between chambers. The leakage past the apex and side seals must be considered when evaluating the combustion performance [2]. The actual burned fuel flow rate $\dot{m}_{fb}$ can be written [4] as

$$\dot{m}_{fb} = \frac{1}{\lambda}[\dot{m}_a - \dot{m}_{leakage} - \frac{\dot{p}_b}{p_b}m_{crevice}] \tag{8}$$

where $\dot{m}_{leakage}$ and $m_{crevice}$ denote the leakage rate and crevice mass of the air-fuel mixture, p_b is the chamber pressure, and $\lambda = \dot{m}_a/\dot{m}_f$ is the air-fuel ratio, which is the control object to be regulated around the stoichiometric value, i.e. $\lambda_d = 14.67$ for petrol. Hence, the indicated engine torque τ_{ind} [13] can be determined as

$$\tau_{ind} = H_u\frac{\eta_{th}(n, p_m, \theta_{SA}, \lambda)\dot{m}_{fb}}{n} \tag{9}$$

where H_u is the fuel energy constant and η_{th} is a complex nonlinear function of the engine speed n, the manifold pressure p_m, the spark advance angle θ_{SA}, and the air-fuel ratio λ.

D. Eccentric shaft model

The eccentric shaft dynamics can be expressed using Newton's second law as

$$J\dot{n} = \tau_{ind} - \tau_{fric} - \tau_{load} \tag{10}$$

where J is the scaled engine moment of inertia, τ_{fric} and τ_{load} refer to the friction and the load torque, respectively [13].

III. Nonlinear Observer Design

It has been shown in our previous work [5] that the AFR regulation problem can be reformulated into a fuel flow tracking problem for the sake of design simplicity. Then the feedback control error e used in the AFR controller can be defined as

$$e = \dot{m}_{fd} - \dot{m}_f = \frac{1}{\lambda_d}\dot{m}_a - \dot{m}_f \tag{11}$$

where $\dot{m}_{fd}$ and λ_d are the desired fuel mass flow rate and AFR. Thus, its derivative is calculated as

$$\dot{e} = \frac{1}{\lambda_d}\ddot{m}_a - \ddot{m}_f \tag{12}$$

Clearly, $\ddot{m}_a$ is the derivative of complex nonlinear air-filling dynamics (5) and $\ddot{m}_f$ is the derivative of (6) with fuel puddle dynamics (7). The measurement of $\ddot{m}_a$ and $\ddot{m}_f$ is practically infeasible. However, it is conceivable to estimate them using nonlinear observers.

This section investigates popular observer techniques from [6] to estimate the dynamics of $\ddot{m}_a$ and $\ddot{m}_f$, which will be used in the AFR control design.

A. Extended Kalman filter

Kalman filters have been widely used as a linear quadratic estimation algorithm, which can be further extended to deal with the nonlinearities [17] and unknown parameters [18]. By inspection of the nonlinear fuel puddle model (6)(7) with the unknown parameters τ and χ, the parameters can be taken as extra states to be estimated. Moreover, it has been shown in [12][16] that the term $\dot{m}_{fpe}$ is negligible. Hence, the fuel puddle process (6)(7) can be written as

$$\begin{cases} \dot{\tau} = w_1 \\ \dot{\chi} = w_2 \\ \dot{m}_{fp} = \chi\dot{m}_{fi} - (1/\tau)m_{fp} + w_3 \\ \dot{m}_{fv} = (1-\chi)\dot{m}_{fi} + (1/\tau)m_{fp} - m_{fv}/\tau_m + w_4 \\ \dot{m}_f = m_{fv}/\tau_m + v \end{cases} \tag{13}$$

or in the form of augmented state equations as

$$\begin{cases} \dot{x} = f(x,u) + w \\ z = h(x) + v \end{cases} \tag{14}$$

where $x = [\tau\ \chi\ m_{fp}\ m_{fv}]^T$ is the augmented state vector, $u = \dot{m}_{fi}$ is the system input (injected fuelling command) and $z = \dot{m}_f$ is the measurement of the system output. Practically, the measurement z can be obtained through dividing the reading of a mass air flow (MAF) sensor by the reading of a lambda sensor since $\dot{m}_f = \dot{m}_a/\lambda$. Moreover, $f(x,u)$ and $h(x)$ denote the nonlinear functions in (13), $w = [w_1\ w_2\ w_3\ w_4]^T \sim \mathcal{N}(0,Q)$ and $v \sim \mathcal{N}(0,R)$ are the zero mean multivariate Gaussian noises that account for the model inaccuracy and sensor noise with pre-defined covariance Q and R.

Assumption 1: It is reasonable in practice to assume that the process noise w and the measurement noise v are bounded, i.e. $||w|| \leq \varpi$ and $|v| \leq \mu$ with $\varpi > 0$ and $\mu > 0$.

For the system (14), an extended Kalman filter can be designed accordingly with the Kalman gain vector K as

$$\dot{\hat{x}} = f(\hat{x},u) + K(z - h(\hat{x})) \tag{15}$$

where $\hat{x}$ is the estimate of the state vector x and K is the adaptive Kalman gain to be designed later.

From (14) and (15), the estimation error is defined as $\tilde{x} = x - \hat{x}$ and its derivative can be written as

$$\begin{aligned} \dot{\tilde{x}} &= \dot{x} - \dot{\hat{x}} \\ &= f(x,u) - f(\hat{x},u) - K(h(x) - h(\hat{x})) + w - Kv \end{aligned} \tag{16}$$

Since f and h are differentiable, the error dynamics can then be linearised around $x, \hat{x}$ such that

$$\dot{\tilde{x}} = (F - KH)\tilde{x} + o(||\tilde{x}||) + w - Kv \tag{17}$$

where $o(||\tilde{x}||)$ denotes the higher order terms of the approximation error, which has an upper bound $\delta > 0$. F and H are the Jacobian matrix of $f(x,u)$ and $h(x)$ with respect to x as

$$F = \frac{\partial f}{\partial x} = \begin{bmatrix} 0 & 0 & 0 & 0 \\ 0 & 0 & 0 & 0 \\ m_{fp}/\tau^2 & u & -1/\tau & 0 \\ -m_{fp}/\tau^2 & -u & 1/\tau & -1/\tau_m \end{bmatrix} \tag{18}$$

$$H = \frac{\partial h}{\partial x} = \begin{bmatrix} 0 & 0 & 0 & 1/\tau_m \end{bmatrix} \tag{19}$$

The Kalman gain K can be online updated by solving the covariance prediction matrix P in the algebraic Riccati equation

$$\dot{P} = FP + PF^T - KHP + Q \tag{20}$$

such that

$$K = PH^TR^{-1} \tag{21}$$

It can be proved that the solution P is bounded and positive definite via Theorem 3.4 in *Optimal Control* [19].

Proposition 1: For the augmented system (14) with the extended Kalman filter (15), the estimation error $\tilde{x}$ will exponentially converge towards a compact set around zero and thus $\hat{x} \to x$ holds provided that the noise/error bounds $\delta \to 0$, $\varpi \to 0$, $\mu \to 0$.

Proof: Defining the inverse of the positive definite matrix P as $Y = P^{-1}$, the algebraic Riccati equation (20) can be transformed into

$$-\dot{Y} = YF + F^TY - YKH + YQY \tag{22}$$

Then a Lyapunov function can be chosen as

$$V_k(t) = \frac{1}{2}\tilde{x}^TY\tilde{x} \tag{23}$$

Its derivative can be calculated using (22) as

$$\begin{aligned}\dot{V}_k(t) &= \frac{1}{2}\dot{\tilde{x}}^T Y\tilde{x} + \frac{1}{2}\tilde{x}^T\dot{Y}\tilde{x} + \frac{1}{2}\tilde{x}^T Y\dot{\tilde{x}} \\ &= -\frac{1}{2}\tilde{x}^T(\dot{Y} + YQY + YKH)\tilde{x} + \frac{1}{2}\tilde{x}^T\dot{Y}\tilde{x} \\ &\quad + \tilde{x}^T Yo(||\tilde{x}||) + \tilde{x}^T Yw - \tilde{x}^T YKv \\ &\leq -\frac{1}{2}\lambda_{\min}(YQY + YKH)||\tilde{x}||^2 \\ &\quad + \frac{\lambda^2_{\max}(Y)}{\sigma}||\tilde{x}||^2 + \frac{\lambda^2_{\max}(YK)}{2\sigma}||\tilde{x}||^2 \\ &\quad + \frac{\sigma}{2}\delta^2 + \frac{\sigma}{2}\varpi^2 + \frac{\sigma}{2}\mu^2 \\ &\leq -a(\sigma)V_k(t) + \beta(\sigma)\end{aligned} \tag{24}$$

where $\lambda_{\min}(\bullet)$, $\lambda_{\max}(\bullet)$ denote the minimum, maximum eigenvalues of a matrix, $a(\sigma) = \lambda_{\min}(YQY + YKH)/\lambda_{\max}(Y) - [2\lambda^2_{\max}(Y) + \lambda^2_{\max}(YK)]/2\sigma\lambda_{\max}(Y)$ and $\beta(\sigma) = \sigma(\delta^2 + \varpi^2 + \mu^2)/2$ are positive constants for a properly chosen constant $\sigma > [2\lambda^2_{\max}(Y) + \lambda^2_{\max}(YK)]/2\lambda_{\min}(YQY + YKH)$. This implies that $V_k(t) \leq V(0)e^{-a(\sigma)t} + \beta(\sigma)/a(\sigma)$ holds and the estimation error $\tilde{x}$ will exponentially converge towards a compact set defined by $\Omega_1 := \{\tilde{x} \mid ||\tilde{x}|| \leq \sqrt{\sigma(\delta^2 + \varpi^2 + \mu^2)/a(\sigma)\lambda_{\min}(Y)}\}$. Clearly, $\lim_{t\to\infty}\tilde{x} = 0$ holds for $\beta(\sigma) \to 0$, i.e. $\delta \to 0$, $\varpi \to 0$, $\mu \to 0$. ◇

Hence, the fuel puddle dynamics as well as the unknown parameters τ and χ can be online estimated via extended Kalman filter (15) using only MAF and lambda sensors.

B. Dirty differentiation observer

In order to formulate the dynamics of the control error, substituting the air-filling dynamics (5) and the fuel puddle dynamics (6)(7) into (12) gives

$$\dot{e} = M - u_d \tag{25}$$

where $M = \frac{V_d}{120R\lambda_d}\frac{d(\eta_{vol}p_m n/T_m)}{dt} - \frac{m_{fp}}{\tau\tau_m} + \frac{m_{fv}}{\tau^2_m}$ is lumped unknown dynamics to be observed and $u_d = (1 - \chi)u/\tau_m$ is a linear function of the control input u with the unknown parameter χ.

An intuitive way to observe the unknown lumped dynamics M is defined in terms of the "the dirty derivative" of e using the low-pass filter operation $(\bullet)_f = [\bullet]/(ks + 1)$, which can be given as

$$\dot{e}_f = \frac{s}{ks+1}e = [\frac{1}{k} - \frac{1}{k(ks+1)}]e \tag{26}$$

where $k > 0$ is the design filter parameter. Then the dirty differentiation observer is designed as

$$\hat{M} = \dot{e}_f + \hat{u}_d \tag{27}$$

with $\hat{u}_d = (1-\hat{\chi})u/\tau_m$, where $\hat{\chi}$ is the estimate of χ using the extended Kalman filter (15). From (25)(26)(27), the estimation error can be written as

$$\tilde{M} = M - \hat{M} = \frac{ks^2}{ks+1}e + \tilde{u}_d \tag{28}$$

with $\tilde{u}_d = u_d - \hat{u}_d$.

Assumption 2: The second derivative of e and the first derivative of $\tilde{x}$ are assumed to be bounded, i.e. $\sup_{t\geq 0}|\ddot{e}(t)| \leq \psi$ and $\sup_{t\geq 0}||\dot{\tilde{x}}(t)|| \leq \zeta$ with $\psi > 0$ and $\zeta > 0$.

Proposition 2: Under Assumption 2, for the error dynamics (25) with the dirty differentiation observer (27) and the extended Kalman filter (15), the estimation errors $\tilde{M}$, $\tilde{x}$ will exponentially converge to a compact set around zero.

Proof: Presenting (28) in the time domain gives

$$\dot{\tilde{M}} = -\tilde{M}/k + \ddot{e} + \dot{\tilde{u}}_d + \tilde{u}_d/k \tag{29}$$

By choosing a Lyapunov function $V_1(t) = \tilde{M}^2/2 + k_1 V_k$ with $k_1 > 0$, it follows that

$$\dot{V}_1(t) = \tilde{M}\dot{\tilde{M}} + k_1\dot{V}_k \leq -a_1(\sigma_1)V_1 + \beta_1(\sigma_1) \tag{30}$$

where $a_1(\sigma_1) = \min\{2/k - 3/\sigma_1, (a(\sigma_1)k_1 - \sigma_1/k^2)/\lambda_{\max}(Y)\}$ and $\beta_1(\sigma_1) = \sigma_1(\psi^2 + \zeta^2)/2 + k_1\beta(\sigma_1)$ are positive constants if the constants σ_1 and k_1 are properly selected as $\sigma_1 > 3k/2$ and $k_1 > \sigma_1/a(\sigma_1)k^2$. This implies $V_1(t) \leq V_1(0)e^{-a_1(\sigma_1)t} + \beta_1(\sigma_1)/a_1(\sigma_1)$ holds and thus $\tilde{M}$, $\tilde{x}$ will exponentially converge towards $\Omega_2 := \{\tilde{M} \mid |\tilde{M}| \leq \sqrt{2\beta_1(\sigma_1)/a_1(\sigma_1)}\}$ and $\Omega_3 := \{\tilde{x} \mid ||\tilde{x}|| \leq \sqrt{2\beta_1(\sigma_1)/a_1(\sigma_1)\lambda_{\min}(Y)}\}$, respectively. ◇

C. Unknown input observer

The unknown input observer [6] is designed based on the idea of using the low-pass filter operation $(\bullet)_f = [\bullet]/(ks+1)$ on both sides of (25) such that

$$\dot{e}_f = M_f - u_{df} \tag{31}$$

Then the unknown input observer can be designed as

$$\hat{M} = M_f = \frac{e - e_f}{k} + \hat{u}_{df} \tag{32}$$

where $e_f, \hat{u}_{df}$ are the filtered version of $e, \hat{u}_d$ as

$$\begin{cases} k\dot{e}_f + e_f = e, & e_f(0) = 0 \\ k\dot{\hat{u}}_{df} + \hat{u}_{df} = \hat{u}_d, & \hat{u}_{df}(0) = 0 \end{cases} \tag{33}$$

with the design filter parameter $k > 0$. From (25)(26)(31)(32), the estimation error can be described as

$$\tilde{M} = M - \hat{M} = \frac{ks}{ks+1}M + \frac{1}{ks+1}\tilde{u}_d \tag{34}$$

Assumption 3: It is practically feasible to assume that the derivative of the lumped unknown term M is bounded, i.e. $\sup_{t\geq 0}|\dot{M}(t)| \leq \xi$ with $\xi > 0$.

Proposition 3: Under Assumption 3, for the error dynamics (25) with the unknown input observer (32) and the extended Kalman filter (15), the estimation errors $\tilde{M}$, $\tilde{x}$ will exponentially converge to a compact set around zero.

Proof: Presenting (34) in the time domain gives

$$\dot{\tilde{M}} = -\tilde{M}/k + \dot{M} + \tilde{u}_d/k \tag{35}$$

By choosing a Lyapunov function $V_2(t) = \tilde{M}^2/2 + k_2 V_k$ with $k_2 > 0$, it follows that

$$\dot{V}_2(t) = \tilde{M}\dot{\tilde{M}} + k_2\dot{V}_k \leq -a_2(\sigma_2)V_2 + \beta_2(\sigma_2) \tag{36}$$

where $a_2(\sigma_2) = \min\{2/k - 2/\sigma_2, (a(\sigma_2)k_2 - \sigma_2/k^2)/\lambda_{\max}(Y)\}$ and $\beta_2(\sigma_2) = \sigma_2\xi^2/2 + k_2\beta(\sigma_2)$ are positive constants if σ_2, k_2 are properly selected as $\sigma_2 > k$, $k_2 > \sigma_2/a(\sigma_2)k^2$. This implies $V_2(t) \le V_2(0)e^{-a_2(\sigma_2)t} + \beta_2(\sigma_2)/a_2(\sigma_2)$ holds and $\tilde{M}$, $\tilde{x}$ will exponentially converge towards $\Omega_4 := \{\tilde{M} \mid |\tilde{M}| \le \sqrt{2\beta_2(\sigma_2)/a_2(\sigma_2)}\}$ and $\Omega_5 := \{\tilde{x} \mid ||\tilde{x}|| \le \sqrt{2\beta_2(\sigma_2)/a_2(\sigma_2)\lambda_{\min}(Y)}\}$, respectively.$\diamond$

Remark 1: The filter operation $(\bullet)_f$ is applied to e for both observers (27) and (32). However, $\hat{u}_d$ is also filtered in (32) while in (27) $\hat{u}_d$ is directly coupled with $\hat{M}$. Furthermore, by inspection of (28) and (34), the estimation error $\tilde{M}$ can be minimized by setting the filter parameter k sufficiently small.

Remark 2: Assumption 3 for the unknown input observer (32) is weaker than Assumption 2 for the dirty differentiation observer (27). For both observers, the upper bound of the estimation error $\tilde{M}$ depends on the convergence bound $\beta(\bullet)$ of the extended Kalman filter (15). For (27), it also depends on the upper bound ψ of the second derivative of e and the upper bound ζ of the first derivative of $\tilde{x}$. In contrast, for (32), it depends only on the upper bound ξ of the first derivative of M apart from $\beta(\bullet)$, which is a weaker condition in practice.

IV. AFR Control Design

Based on the observers above, the injected fuel mass flow rate for AFR control can be designed as

$$u = \dot{m}_{fi} = \tau_m(k_p e + \hat{M})/(1-\hat{\chi}) \tag{37}$$

where $k_p > 0$ is the feedback gain to be tuned, $\hat{\chi}$ and $\hat{M}$ are the estimates of χ and M via the extended Kalman filter (15) and the unknown input observer (32), respectively.

Theorem 1: For the Wankel engine model given in Section II and the error dynamics (25), the AFR control (37) based on the extended Kalman filter (15) and the unknown input observer (32) will lead to the exponential convergence of the error e and the estimation errors $\tilde{M}$, $\tilde{x}$ towards a small compact set around zero.

Proof: Substituting (37) into $u_d = (1-\chi)u/\tau_m$ gives

$$\begin{aligned} u_d &= (1-\chi)(k_p e + \hat{M})/(1-\hat{\chi}) \\ &= \tilde{\chi}(k_p e + \hat{M})/(1-\hat{\chi}) + (k_p e + \hat{M}) \end{aligned} \tag{38}$$

with $\tilde{\chi} = \chi - \hat{\chi}$. Then the closed-loop error dynamics can be calculated by substituting (38) into (25) as

$$\dot{e} = -k_p e + \tilde{M} - \tilde{\chi}(k_p e + \hat{M})/(1-\hat{\chi}) \tag{39}$$

Selecting a Lyapunov function as

$$W(t) = e^2/2 + k_3\tilde{M}^2/2 + k_4\tilde{x}^T Y\tilde{x}/2 \tag{40}$$

with $k_3 > 0$, $k_4 > 0$ to be chosen, its first derivative can be determined using (24)(36)(39) as

$$\begin{aligned} \dot{W}(t) &= e\dot{e} + k_3\dot{V}_2 + k_4\dot{V}_k \\ &\le -[k_p - \epsilon(k_p^2 e^2 + \hat{M}^2)/2(1-\hat{\chi})^2 - \epsilon/2]e^2 \\ &\quad - (k_3/k - k_3/\epsilon - 1/2\epsilon)\tilde{M}^2 \\ &\quad - [(k_2k_3 + k_4)a(\epsilon) - \epsilon k_3/2k^2 - 2/\epsilon]||\tilde{x}||^2/2 \\ &\quad + k_3\beta_2(\epsilon) + k_4\beta(\epsilon) \\ &\le -bW(t) + \Delta \end{aligned} \tag{41}$$

where $b = \min\{2k_p - \epsilon(k_p^2 e^2 + \hat{M}^2)/(1-\hat{\chi})^2 - \epsilon,\ 2(k_1/k - k_3/\epsilon - 1/2\epsilon),\ (k_2k_3a(\epsilon) + k_4a(\epsilon) - \epsilon k_3/2k^2 - 2/\epsilon)/\lambda_{\max}(Y)\}$ and $\Delta = k_3\beta_2(\epsilon) + k_2\beta(\epsilon)$ are positive constants if k_p, k_3, k_4 are properly selected as $k_p > \epsilon(k_p^2 e^2 + \hat{M}^2)/2(1-\hat{\chi})^2 - \epsilon/2$, $k_3 > k/2(\epsilon - k)$, $k_4 > \epsilon k_3/2a(\epsilon)k^2 + 2/a(\epsilon)\epsilon - k_2k_3a(\epsilon)$ with a constant $\epsilon > 0$. This implies that $W(t) \le W(0)e^{-bt} + \Delta/b$ holds and then e, $\tilde{M}$ will exponentially converge towards $\Omega_6 := \{\Psi \mid |\Psi| \le \sqrt{2\Delta/b}\}$ and $\tilde{x}$ will exponentially converge towards $\Omega_7 := \{\tilde{x} \mid ||\tilde{x}|| \le \sqrt{2\Delta/b\lambda_{\min}(Y)}\}$. $\diamond$

Remark 3: Similar to Theorem 1, the control (37) with the dirty differentiation observer (27) can be addressed in the same manner via Proposition 2.

In practice, the control error e in (37) can be obtained from (11), where $\dot{m}_a$ is measured by a MAF sensor and $\dot{m}_f$ is calculated using MAF and lambda sensors as $\dot{m}_f = \dot{m}_a/\lambda$. By Theorem 1, the fuel mass flow rate $\dot{m}_f$ can track the desired reference $\dot{m}_{fd}$ and thus the AFR λ is regulated around the stoichiometric value λ_d.

V. Simulations

In this section, the Wankel engine dynamics in section II are modelled and created in MatLab/Simulink, where the model parameters are calibrated based on the experimental data sets [1][5][13]. The throttle angle is controlled to operate the engine with fair acceleration and deceleration.

A. Fuel puddle estimation

The fuel puddle dynamics (13) are estimated using the extended Kalman filter (15). Sufficient Gaussian noises are added into the measurement of AFR λ and air mass flow rate $\dot{m}_a$ to account for the effect of sensor noise. Fig. 1 presents the simulation results of the estimated and measured AFR. The extended Kalman filter performs satisfactory estimation for both transients and steady states. Moreover, the unknown parameter τ and χ can quickly converge to the true value $\tau = 2.5$s and $\chi = 0.6$, which is shown in Fig. 2.

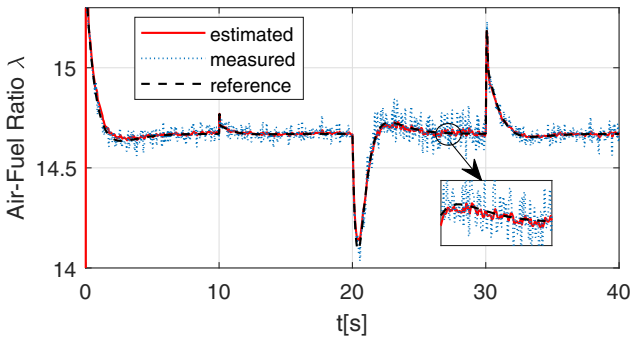

Fig. 1: Comparison between the estimated and measured AFR.

B. Air-fuel ratio control

The proposed AFR control based on the two observers (27)(32) are compared with a fixed-gain PID controller, of which the simulation results are provided in Fig. 3. It is obvious that all the controllers are able to regulate the AFR at the

stoichiometric value $\lambda_d = 14.67$ in steady states. For transients (e.g. $t = 10,\ 20,\ 30$s when engine accelerates/decelerates), both observer-based controllers (b)(c) to some extent reduce the transient errors compared to the PID controller (a) in Fig. 3. However, the controller based on the dirty differentiation observer (27) appears to be slower at transients. It is clear that the controller based on the unknown input observer (32) achieves better robustness against disturbances.

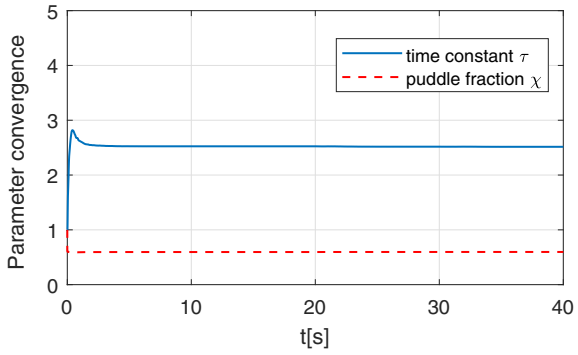

Fig. 2: Convergence of the estimated fuel puddle parameters.

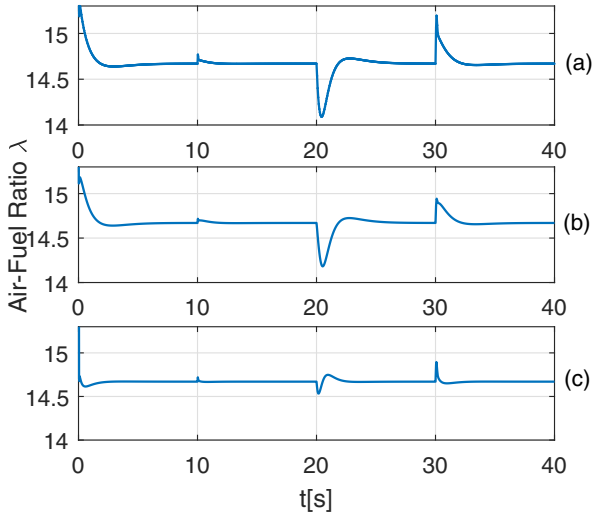

Fig. 3: Comparison of the AFR responses based on (a) PID control, (b) dirty differentiation observer (27), and (c) unknown input observer (32).

VI. Conclusions

In this paper, a dedicated model of Wankel engine dynamics was first developed for the design of different nonlinear observers and AFR control. The regulation of AFR was first reformulated into a fuel mass flow rate tracking problem. As a widespread issue for PFI engines, the nonlinear fuel puddle dynamics were online estimated using an extended Kalman filter by taking the unknown parameters as augmented states. The complex air-filling dynamics were lumped and estimated using novel observer techniques. Then a feedback control was designed combining the observers to stablize the AFR. Comparative numerical simulations validated that the proposed method can regulate the AFR around the stoichiometric value at both transients and steady states, where the newly proposed unknown input observer demonstrates better robustness against disturbances. Future work will focus on the implementation of the proposed controller on a practical Wankel engine.

References

[1] M. Peden, M. Turner, J. W. G. Turner, and N. Bailey, "Comparison of 1-d modelling approaches for wankel engine performance simulation and initial study of the direct injection limitations," SAE Technical Paper 2018-01-1452, Tech. Rep., 2018.

[2] R. Sierens, R. Baert, D. Winterbone, and P. Baruah, "A comprehensive study of wankel engine performance," SAE Technical Paper, Tech. Rep., 1983.

[3] L. Tartakovsky, V. Baibikov, M. Gutman, M. Veinblat, and J. Reif, "Simulation of wankel engine performance using commercial software for piston engines," SAE Technical Paper, Tech. Rep., 2012.

[4] T. J. Norman, "A performance model of a spark ignition wankel engine: including the effects of crevice volumes, gas leakage, and heat transfer," Ph.D. dissertation, Massachusetts Institute of Technology, 1983.

[5] A. S. Chen, J. Na, G. Herrmann, R. Burke, and C. Brace, "Adaptive air-fuel ratio control for spark ignition engines with time-varying parameter estimation," in *Modelling, Identification and Control (ICMIC), 2017 9th International Conference on*. IEEE, 2017, pp. 1074–1079.

[6] J. Na, G. Herrmann, C. Rames, R. Burke, and C. Brace, "Air-fuel-ratio control of engine system with unknown input observer," in *Control (CONTROL), 2016 UKACC 11th International Conference on*. IEEE, 2016, pp. 1–6.

[7] J. Yang, T. Shen, and X. Jiao, "Model-based stochastic optimal air–fuel ratio control with residual gas fraction of spark ignition engines," *IEEE Transactions on Control Systems Technology*, vol. 22, no. 3, pp. 896–910, 2014.

[8] R. A. Zope, J. Mohammadpour, K. M. Grigoriadis, and M. Franchek, "Air-fuel ratio control of spark ignition engines with twc using lpv techniques," in *ASME 2009 Dynamic Systems and Control Conference*. American Society of Mechanical Engineers, 2009, pp. 897–903.

[9] S. Wang and D. Yu, "A new development of internal combustion engine air-fuel ratio control with second-order sliding mode," *Journal of Dynamic Systems, Measurement, and Control*, vol. 129, no. 6, pp. 757–766, 2007.

[10] Y. Yildiz, A. M. Annaswamy, D. Yanakiev, and I. Kolmanovsky, "Spark ignition engine fuel-to-air ratio control: An adaptive control approach," *Control Engineering Practice*, vol. 18, no. 12, pp. 1369–1378, 2010.

[11] S. B. Choi and J. K. Hedrick, "An observer-based controller design method for improving air/fuel characteristics of spark ignition engines," *IEEE Transactions on Control Systems Technology*, vol. 6, no. 3, pp. 325–334, 1998.

[12] I. Arsie, C. Pianese, G. Rizzo, and V. Cioffi, "An adaptive estimator of fuel film dynamics in the intake port of a spark ignition engine," *Control Engineering Practice*, vol. 11, no. 3, pp. 303–309, 2003.

[13] E. Hendricks and J. B. Luther, "Model and observer based control of internal combustion engines," in *Proceedings of International Workshop on Modeling, Emissions and Control in Automotive Engines (MECA01)*. Citeseer, 2001.

[14] E. Hendricks, A. Chevalier, M. Jensen, S. C. Sorenson, D. Trumpy, and J. Asik, "Modelling of the intake manifold filling dynamics," SAE Technical Paper, Tech. Rep., 1996.

[15] G. A. Danieli, J. C. Keck, and J. B. Heywood, "Experimental and theoretical analysis of wankel engine performance," SAE Technical Paper, Tech. Rep., 1978.

[16] I. Arsie, F. De Franceschi, C. Pianese, and G. Rizzo, "Odecs-a computer code for the optimal design of si engine control strategies," SAE Technical Paper, Tech. Rep., 1996.

[17] S. J. Julier and J. K. Uhlmann, "New extension of the kalman filter to nonlinear systems," in *Signal processing, sensor fusion, and target recognition VI*, vol. 3068. International Society for Optics and Photonics, 1997, pp. 182–194.

[18] L. Ljung, "Asymptotic behavior of the extended kalman filter as a parameter estimator for linear systems," *IEEE Transactions on Automatic Control*, vol. 24, no. 1, pp. 36–50, 1979.

[19] F. L. Lewis, D. Vrabie, and V. L. Syrmos, *Optimal control*. John Wiley & Sons, 2012.